SRO9, a Multicopy Suppressor of the Bud Growth Defect in the *Saccharomyces cerevisiae rho3*-Deficient Cells, Shows Strong Genetic Interactions With Tropomyosin Genes, Suggesting Its Role in Organization of the Actin Cytoskeleton

Mitsuhiro Kagami, Akio Toh-e and Yasushi Matsui

Department of Biological Sciences, Graduate School of Science, The University of Tokyo, Hongo, Tokyo 113, Japan

Manuscript received March 26, 1997
Accepted for publication July 10, 1997

ABSTRACT

RHO3 encodes a Rho-type small GTPase in the yeast *Saccharomyces cerevisiae* and is involved in the proper organization of the actin cytoskeleton required for bud growth. *SRO9* (*YCL37c*) was isolated as a multicopy suppressor of a *rho3*Δ mutation. An Sro9p domain required for function is similar to a domain in the La protein (an RNA-binding protein). Disruption of *SRO9* did not affect vegetative growth, even with the simultaneous disruption of an *SRO9* homologue, *SRO99*. However, *sro9*Δ was synthetically lethal with a disruption of *TPM1*, which encodes tropomyosin; *sro9*Δ *tpm1*Δ cells did not distribute cortical actin patches properly and lysed. We isolated *TPM2*, the other gene for tropomyosin, as a multicopy suppressor of a *tpm1*Δ *sro9*Δ double mutant. Genetic analysis suggests that *TPM2* is functionally related to *TPM1* and that tropomyosin is important but not essential for cell growth. Overexpression of *SRO9* suppressed the growth defect in *tpm1*Δ *tpm2*Δ cells, disappearance of cables of actin filaments in both *rho3*Δ cells and *tpm1*Δ cells, and temperature sensitivity of actin mutant cells (*act1-1* cells), suggesting that Sro9p has a function that overlaps or is related to tropomyosin function. Unlike tropomyosin, Sro9p does not colocalize with actin cables but is diffusely cytoplasmic. These results suggest that Sro9p is a new cytoplasmic factor involved in the organization of actin filaments.

THE actin cytoskeleton mediates many essential processes for cell functions, such as the transport of secretory vesicles, morphogenetical changes of cells, the intracellular movement of the organelles, the structural integrity of the cells, and cytokinesis. In budding yeast, the actin cytoskeleton is distributed asymmetrically; cortical actin patches are at the sites of surface growth and actin cables are oriented along the axis of formation of the bud (Adams and Pringle 1984; Kilmartin and Adams 1984), suggesting that they have a role in directing materials for new cell wall and membrane to growing portions of the cells. Mutations in the essential actin gene (*ACT1*) result in an inability to undergo apical growth and in defects in secretion (at the late stages, Golgi to plasma membrane) (Novick and Botstein 1985).

The actin cytoskeleton requires many associated proteins, including tropomyosin (Bretscher *et al.* 1994; Welch *et al.* 1994). Tropomyosin regulates the interaction between myosin and actin in muscle cells (Cummins and Perry 1974). In yeast cells, tropomyosin, encoded by *TPM1* and *TPM2*, binds to and stabilizes actin cables (Liu and Bretscher 1989; Drees *et al.* 1995) and is suggested to be involved in membrane trafficking since *tpm1*Δ cells exhibit accumulation of membrane vesicles (Liu and Bretscher 1992).

Corresponding author: Yasushi Matsui, Department of Biological Sciences, The University of Tokyo, 7-3-1, Hongo, Bunkyo-ku, Tokyo 113, Japan. E-mail: matsui@biol.s.u-tokyo.ac.jp

Accumulating evidence indicates that the organization of actin filaments and the morphological change depending on the actin cytoskeleton are regulated by rho-type GTPases (Hall 1992, 1994; Ridley 1995; Takai *et al.* 1995). The yeast *Saccharomyces cerevisiae* possesses six rho-type GTPases: *RHO1, 2, 3, 4, YNL180c* (should be referred to *RHO5*), and *CDC42* (Madaule *et al.* 1987; Johnson and Pringle 1990; Matsui and Toh-e 1992a). Both *RHO1* and *CDC42* are essential, and *RHO3* is nearly essential for cell growth (Madaule *et al.* 1987; Johnson and Pringle 1990; Matsui and Toh-e 1992a). *RHO4* is functionally related to *RHO3* since disruption of *RHO4* enhances the defect of *rho3*Δ cells and *RHO4* can serve as a multicopy suppressor of *rho3*Δ (Matsui and Toh-e 1992a). Cells depleted for Rho3p undergo lysis with a small bud, and temperature-sensitive *rho3* cells lose cell polarity during bud formation and grow more isotropically than wild-type cells at nonpermissive temperatures (Matsui and Toh-e 1992b). Cells expressing dominant active mutant *RHO3* become elongated and bent, often at the position where actin patches are abnormally concentrated (Imai *et al.* 1996). These phenotypes suggest that Rho3p directs organization of the actin cytoskeleton and modulates morphogenesis during bud growth.

We have identified genes that, when overexpressed, suppress the *rho3*Δ defect, such as *RHO4, SRO1* (*BEM1*), *SRO2* (*CDC42*), *SRO6* (*SEC4*), and other *SRO* genes (*SRO3, 4, 5, 7, 8,* and *9*) (Matsui and Toh-e

1992b; IMAI *et al.* 1996). Both Cdc42p and Bem1p are required for cell polarization in bud formation, as well as in the formation of mating projections, and Bem1p interacts with factors involved in the morphogenesis, including actin (JOHNSON and PRINGLE 1990; BENDER and PRINGLE 1991; CHENEVERT *et al.* 1992; LEEUW *et al.* 1995; BENDER *et al.* 1996; MATSUI *et al.* 1996). *SEC4* is essential for the fusion of secretory vesicles with plasma membrane (NOVICK and SCHEKMAN 1979; SALMINEN and NOVICK 1987) and the fusion for exocytosis is important for bud growth since exocytosis is restricted to occur at a bud in growing cells (TKACZ and LAMPEN 1972; FIELD and SCHEKMAN 1980). These facts suggest that genes that can serve as a multicopy suppressor of *rho3*Δ are the strong candidates for the genes that play an important role in morphogenesis during bud growth.

In this article, we have characterized *SRO9* and found strong genetic interactions among *TPM1, ACT1, RHO3,* and *SRO9*. *SRO9* can compensate for the loss of tropomyosin. The genetic analysis of *SRO9* in this article suggests that Sro9p is involved in polarized organization of actin cytoskeleton.

MATERIALS AND METHODS

Microbiological techniques: Yeast transformations were performed by the method of ITO *et al.* (1983). Rich medium containing glucose (YPD) and synthetic minimal medium (SD) were as described (SHERMAN *et al.* 1986). SC contains 0.5% casamino acids (Difco) and 100 mg/liter each of uracil, adenine sulfate, and tryptophan in SD. SC −U is SC lacking uracil. SC −W is SC lacking tryptophan. YPGal is YPD except that 2% glucose is replaced with 5% galactose and 0.3% sucrose. SCGal −U is SC −U except that 2% glucose is replaced with 5% galactose and 0.3% sucrose. Doubling time of cells with a plasmid was calculated from the measurement of optical density 600 nm in log-phase cultures of three independent transformants.

Strains and plasmids: The yeast strains used are listed in Table 1. The *Escherichia coli* strain used is strain DH5α [*supE44 ΔlacU169 (φ80lacZΔm15) hsdR17 recA1 endA1 gyrA96 thi-1 relA1*]. Plasmid DNA was prepared as described by MANIATIS *et al.* (1982). Yeast DNA was prepared as described by SHERMAN *et al.* (1986). Plasmid pSRO9, carrying *SRO9*, is an original isolate (MATSUI and TOH-E 1992b) from a yeast genomic library based on the high-copy number plasmid YEp24 (CARLSON and BOTSTEIN 1982). pSRO9-1 was constructed by removing the *Sph*I (in YEp24)-*Bst*EII fragment from pSRO9. pSRO9 was digested with *Sal*I and religated to construct pSRO9-2. pSRO9-3 was constructed by removing the *Sph*I (in YEp24)-*Sac*I fragment from pSRO9. pSRO9-4 was constructed by removing the *Sma*I (in YEp24)-*Sac*I fragment from pSRO9. pSRO9 was digested with *Sac*II and then religated after removing the overhang of the *Sac*II cleavage site using T4 DNA polymerase to construct pSRO9-5. To construct YEpWSRO9, the 1.8-kb *Xho*I-*Eco*RI fragment from pSRO9 was inserted between the *Sal*I and *Eco*RI sites of a high-copy number plasmid YEplac112 (GIETZ and SUGINO 1988). pUCSRO9 and KS$^+$SRO9 were constructed by inserting the 2.5-kb *Bgl*II fragment from pSRO9 into the *Bam*HI site of pUC119 (VIEIRA and MESSING 1987) and pBluescript KS$^+$ (Stratagene La Jolla, CA), respectively. For the disruption of *SRO9*, pSRO9Δ was constructed by replacing the 0.9-kb *Stu*I fragment of KS$^+$SRO9 with a 1.4-kb *HIS3* fragment. pSRO9Δ was digested with *Spe*I and *Sal*I for replacement transformation. Using this construct, the *SRO9* region from the 117th codon to 2 bp downstream of the stop codon is replaced with *HIS3* (*sro9*Δ*::HIS3*).

YIpUGAL7, an integration vector carrying the *URA3* marker (MATSUI and TOH-E 1992b), was digested with *Eco*RI and then religated after filling up the overhang using the Klenow fragment of *E. coli* DNA polymerase I to construct YIpUGAL7ΔRI. YIpUGAL7RI was constructed by inserting a *Eco*RI linker into the *Bgl*II site, located at the downstream of the *GAL7* promoter, of YIpUGAL7ΔRI after filling up the overhang of the *Bgl*II cleavage site by the Klenow fragment. The complete *SRO9* coding region was amplified by polymerase chain reaction (PCR; SAIKI *et al.* 1988) using the two convergent primers, 5′-GGGGGGAATTCATGAAGATCTTTTGGGGA and 5′-TTATGATGATAATGTAC. The amplified fragment was digested with *Eco*RI in the primer and 3′-noncoding region of *SRO9* (see Figure 1A) and inserted into the *Eco*RI site of YIpUGAL7RI to create YIpUGAL7SRO9. YIpUGAL7SRO9 was digested with *Apa*I and introduced into cells to be integrated at the *ura3* locus. After the integration, the *URA3* marker was replaced with *LEU2* by a *ura3*-disruption plasmid (MATSUI and TOH-E 1992b). From the construct, *SRO9* is expressed under the control of the *GAL7* promoter and is designated *pGAL7:SRO9*.

pRS316-SRO9 was constructed by inserting the 1.8-kb *Xho*I-*Eco*RI fragment from pSRO9 between the *Xho*I and *Eco*RI sites of a low-copy number plasmid pRS316 (SIKORSKI and HIETER 1989). pRS316-SRO9ΔHB, carrying the truncated version of *SRO9* (*sro9-ΔHB*, see Figure 1), was constructed by replacing the *Hpa*I-*Bal*I fragment of pRS316-SRO9 with a *Hin*dIII linker (8mer). In this construct, the region for Sro9p between the 293rd residue and the 338th residue was deleted in frame. YEplac195-SRO9ΔHB was constructed by inserting the 1.6-kb *Xho*I-*Eco*RI fragment from pRS316-SRO9ΔHB between the *Sal*I and *Eco*RI sites of a high-copy number plasmid YEplac195 (GIETZ and SUGINO 1988).

YEpWSRO99, a high-copy-number plasmid carrying *SRO99* (see RESULTS), was constructed as follows. The 3′-noncoding region (from 55 to 957 bp downstream of the stop codon) of *SRO99* was amplified by PCR using the two convergent primers, 5′-GGGGGGGATCCATAAGATATTTATATAGAGG and 5′-GGGGGAAGCTTTTGGTACTGGTACTAACGGT. The amplified fragment was digested with *Bam*HI and *Hin*dIII and inserted between the *Bam*HI and *Hin*dIII sites of pRS306 (SIKORSKI and HIETER 1989). The resultant plasmid was digested with *Sph*I and introduced into yeast cells (strain YPH499) to be integrated at the downstream of the *SRO99* locus. The genomic DNA of this transformant was digested with *Eco*T22I, ligated, and introduced into *E. coli* cells to isolate a circularized plasmid, pRS306-SRO99, containing a 3.2-kb fragment bearing *SRO99*. The 3.2-kb *Eco*T22I-*Hin*dIII DNA fragment from pRS306-SRO99 was inserted between the *Pst*I and *Hin*dIII sites of YEplac112 to construct YEpWSRO99. For the disruption of *SRO99*, the 3.2-kb *Bam*HI-*Hin*dIII fragment from YEpWSRO99 was inserted between the *Bam*HI and *Hin*dIII sites of pBluescript KS$^+$ and the 1.2-kb *Bgl*II fragment in the resultant plasmid was replaced by a 1.1-kb *URA3* fragment to create pSRO99Δ. pSRO99Δ was digested with *Pvu*II for replacement transformation. Using this construct, the *SRO99* region, containing the 289-bp upstream region of the *SRO99* coding region and the region for the N-terminal half (1–295 amino acids) in the open reading frame of 447 amino acids, is replaced with *URA3* (*sro99*Δ*::URA3*).

pTPM2, carrying *TPM2*, was isolated from a yeast genomic library based on YEp24 (CARLSON and BOTSTEIN 1982) as a multicopy suppresser of *sro9*Δ *tpm1*Δ defect (see RESULTS).

TABLE 1

Yeast strains used in this study

Strain	Genotype	Reference or source
YPH499	*MAT***a** *ura3-52 leu2 his3 trp1 lys2 ade2*	Sikorski and Hieter (1989)
YPH500	*MATα ura3-52 leu2 his3 trp1 lys2 ade2*	Sikorski and Hieter (1989)
YPH501	*MAT***a***/MATα ura3-52/ura3-52 leu2/leu2 his3/his3 trp1/trp1 lys2/lys2 ade2/ade2*	Sikorski and Hieter (1989)
YMR505	*MATα rho3Δ::LEU2 pGAL7:RHO4:HIS3* (in *ura3* locus) *leu2 his3 trp1 lys2 ade2*	Matsui and Toh-e (1992b)
YMR420	*MAT***a** *cdc42-1 ura3 leu2 his3 trp1 lys2 ade2*	Matsui and Toh-e (1992b)
YMR3732-2B	*MATα rho3-1:TRP1 ura3 leu2 his3 trp1 lys2 ade2*	Imai *et al.* (1996)
YMK007	*MATα bem1Δ::URA3 ura3-52 leu2 his3 trp1 lys2 ade2*	A segregant of YPH501 transformed with pBEM1Δ
YMK011A	*MAT***a** *sro9Δ::HIS3 ura3-52 leu2 his3 trp1 lys2 ade2*	A segregant of YPH501 transformed with pSRO9Δ
YMK011B	*MATα sro9Δ::HIS3 ura3-52 leu2 his3 trp1 lys2 ade2*	A segregant of YPH501 transformed with pSRO9Δ
YMK011C	*MAT***a***/MATα sro9Δ::HIS3/sro9Δ::HIS3 ura3-52/ura3-52 leu2/leu2 his3/his3 trp1/trp1 lys2/lys2 ade2/ade2*	YMK011A × YMK011B
YMK012	*MAT***a***/MATα sro9Δ::HIS3/sro9Δ::HIS3 tpm1Δ::URA3/TPM1 ura3-52/ura3-52 leu2/leu2 his3/his3 trp1/trp1 lys2/lys2 ade2/ade2*	YMK011C transformed with a *tpm1*-disruption plasmid (Liu and Bretscher 1989)
YMK013	*MATα sro99Δ::URA3 ura3-52 leu2 his3 trp1 lys2 ade2*	A segregant of YPH501 transformed with pSRO99Δ
YMK014	*MATα tpm1Δ::URA3 ura3-52 leu2 his3 trp1 lys2 ade2*	A segregant of YPH501 transformed with a *tpm1*-disruption plasmid (Liu and Bretscher 1989)
YMK014-1	*MATα tpm1Δ::LEU2 ura3-52 leu2 his3 trp1 lys2 ade2*	YMK014 transformed with a *ura3*-disruption plasmid
YMK015	*MAT***a***/MATα sro9Δ::HIS3/SRO9 tpm1Δ::URA3/TPM1 pGAL7:SRO9:LEU2* (in *ura3* locus) *ura3/ura3-52 leu2/leu2 his3/his3 trp1/trp1 lys2/lys2 ade2/ade2*	A diploid cell (YMK019 × YPH499) transformed with a *tpm1*-disruption plasmid (Liu and Bretscher 1989)
YMK016	*MATα pGAL7:SRO9:LEU2* (in *ura3* locus) *ura3 leu2 his3 trp1 lys2 ade2*	A segregant of YMK015
YMK017	*MATα tpm1Δ::URA3 pGAL7:SRO9:LEU2* (in *ura3* locus) *ura3 leu2 his3 trp1 lys2 ade2*	A segregant of YMK015
YMK017-1	*MATα tpm1Δ::TRP1 pGAL7:SRO9:LEU2* (in *ura3* locus) *ura3 leu2 his3 trp1 lys2 ade2*	YMK017 transformed with a *ura3*-disruption plasmid
YMK018	*MATα sro9Δ::HIS3 tpm1Δ::URA3 pGAL7:SRO9:LEU2* (in *ura3* locus) *ura3 leu2 his3 trp1 lys2 ade2*	A segregant of YMK015
YMK018-1	*MATα sro9Δ::HIS3 tpm1Δ::TRP1 pGAL7:SRO9:LEU2* (in *ura3* locus) *ura3 leu2 his3 trp1 lys2 ade2*	YMK018 transformed with a *ura3*-disruption plasmid
YMK019	*MATα sro9Δ::HIS3 pGAL7:SRO9:LEU2* (in *ura3* locus) *ura3 leu2 his3 trp1 lys2 ade2*	YMK011B integrated *pGAL7:SRO9:LEU2*
YMK020	*MAT***a***/MATα tpm1Δ::LEU2/TPM1 tpm2Δ::URA3/TPM2 ura3-52/ura3-52 leu2/leu2 his3/his3 trp1/trp1 lys2/lys2 ade2/ade2*	A diploid cell (YMK014-1 × YPH499) transformed with pTPM2Δ
YMK020-4A	*MAT***a** *ura3-52 leu2 his3 trp1 lys2 ade2*	A segregant of YMK020
YMK020-4B	*MAT***a** *tpm1Δ::LEU2 tpm2Δ::URA3 ura3-52 leu2 his3 trp1 lys2 ade2*	A segregant of YMK020
YMK020-4C	*MATα tpm2Δ::URA3 ura3-52 leu2 his3 trp1 lys2 ade2*	A segregant of YMK020
YMK020-4D	*MATα tpm1Δ::LEU2 ura3-52 leu2 his3 trp1 lys2 ade2*	A segregant of YMK020
JP7A	*MATα myo2-66 ura3-52 leu2-3,112 his6 ade1*	Johnston *et al.* (1991)
YMK021	*MATα myo2-66 ura3-52 leu2*	Derived from a series of back crosses of JP7A to YPH499
DDY176	*MAT***a** *act1-1 ura3 leu2 his4 trp1*	From D. Drubin (University of Calfornia, Berkeley)
YMK022	*MATα act1-1 ura3 leu2 trp1*	Derived from a series of back crosses of DDY176 to YPH500
DDY177	*MAT***a** *act1-2 ura3 leu2 his4 trp1*	From D. Drubin (University of Calfornia, Berkeley)
YMK023	*MATα act1-2 ura3 leu2 trp1*	Derived from a series of back crosses of DDY177 to YPH500
YJS4-2A	*MAT***a** *sec4-2 ura3 leu2 his3 trp1 lys2 ade2*	Imai *et al.* (1996)
YMK024	*MATα myo1Δ::LEU2 ura3-52 leu2 his3 trp1 lys2 ade2*	A segregant of YPH501 transformed with pMYO1Δ

All strains listed above, except for JP7A, DDY176, and DDY177 strains, are in the YPH499 background. For YMK021, YMK022 and YMK023, only relevant genotypes are described.

YEpLTPM2 and YEpUTPM2 were constructed by inserting the 1.5-kb *Eco*T22I-*Eco*RV fragment from pTPM2 between the *Pst*I and *Sma*I sites of high-copy-number plasmids, YEplac181 and YEplac195 (GIETZ and SUGINO 1988), respectively. pUCTPM2 was constructed by inserting the 2.5-kb *Bam*HI-*Hinc*II fragment from pTPM2 between the *Bam*HI and *Hinc*II site of pUC119. For the disruption of *TPM2,* pUCTPM2Δ was constructed by replacing the 0.9-kb *Eco*RV-*Bgl*II fragment in pUCTPM2 with a 1.1-kb *URA3* fragment. pUCTPM2Δ was digested with *Pvu*II for replacement transformation. Using this construct, the *TPM2* region between 658 bp upstream of the *TPM2* coding region and the 127th codon is replaced with *URA3* (*tpm2Δ::URA3*). *TPM1* was disrupted with a *tpm1*-disruption plasmid (LIU and BRETSCHER 1989) and the disrupted allele is designated *tpm1Δ::URA3.* The *URA3* marker in *tpm1Δ::URA3* was replaced, using *ura3*-disruption plasmids, with the *TRP1* marker or *LEU2* marker (*tpm1Δ::TRP1* and *tpm1Δ::LEU2,* respectively).

For disruption of *BEM1,* the 3.3-kb *Sma*I (in the 5′-noncoding region of *BEM1*)-*Bam*HI (in the 3′-noncoding region of *BEM1*) fragment was inserted between the *Hinc*II and *Bam*HI sites of pBluescript KS^+, and the 1.6-kb *Hin*dIII (in the coding region of *BEM1*)-*Hin*dIII (in the 3′-noncoding region of *BEM1*) fragment in the resultant plasmid was replaced with a 1.1-kb *URA3* fragment to create pBEM1Δ, carrying *bem1Δ::URA3.* pBEM1Δ was digested with *Xho*I and *Bam*HI for replacement transformation.

The plasmid for disruption of *MYO1* was constructed as follows. A 1.2-kb fragment, carrying 3′-half of the coding region (including a *Eco*RV site) and 3′-noncoding region (including a *Eco*RV site) of *MYO1,* was amplified by PCR using a set of primers (5′-GATGCGCTGCAGATATCAAACGCAGCA and 5′-GCCAGATGATATCTCACGTGTTGCCGA). The amplified fragment was digested with *Eco*RV and inserted into the *Sma*I site of pRS305 (SIKORSKI and HIETER 1989) to create pRS305-M3. A 1.9-kb fragment, carrying 5′-half of the coding region (including a *Hin*dIII site) and 5′-noncoding region (including a *Pst*I site) of *MYO1,* was amplified by PCR using a set of primers (5′-CAAGGTCATGGCTTTTAAACAAAGCGT and 5′-CGTTCCTAGATTTAAGGCGATGAT). The amplified fragment was digested with *Hin*dIII and *Pst*I and inserted between the *Hin*dIII and *Pst*I sites of pRS305-M3 to create pMYO1Δ. pMYO1Δ was digested with *Pst*I for replacement transformation. Using this construct, the *MYO1* region between the 220th codon and the 1700th codon (based on the *MYO1* sequence in Saccharomyces Genome Database) is replaced with pRS305 DNA (designated *myo1Δ::LEU2*). All disruptions were confirmed by Southern analysis.

Suppression of *rho3*: A *rho3Δ* disruptant (strain YMR505), which carries *pGAL7:RHO4* (*RHO4* under the control of the *GAL7* promoter), grows poorly on glucose-containing medium, but grows well on galactose-containing medium because *RHO4* can serve as a multicopy suppressor of *rho3Δ* (MATSUI and TOH-E 1992a). Plasmids were introduced into YMR505 on galactose-containing medium and the transformants were streaked on YPD plates and incubated for 3 days at 30°.

Anti-Sro9p antisera: The 1.6-kb *Eco*RI fragment from pUC-SRO9, carrying the *SRO9* coding region, was inserted into the *Eco*RI site of pGEXKG vector for production of glutathione-*S*-transferase (GST)-fused Sro9p in *E. coli* (GUAN and DIXON 1991). Purification of the GST-fused protein was performed as described previously (SHIRAYAMA *et al.* 1995). The purified GST-fused Sro9p was used as an antigen to raise anti-Sro9p antibodies in rabbits.

Cell lysis assay: Cell lysis was assayed by monitoring the leakage of alkaline phosphatase, a yeast intracellular protein, into the culture medium by the method described (PARAVICINI *et al.* 1992). Cells were streaked on YPD plates and incubated at 25° for 2–3 days. The plates were overlaid with BCIP solution (10 mM 5-bromo-4-chloro-3-indolyl phosphate, 0.1 M Tris-HCl pH 9.5 and 1% agar) and incubated for appropriate time at room temperature.

Isolation of multicopy suppressor of *sro9Δ tpm1Δ*: *sro9Δ tpm1Δ pGAL7:SRO9* cells (strain YMK018-1) were transformed with a yeast genomic DNA library constructed in the high-copy-number plasmid YEp24 (CARLSON and BOTSTEIN 1982) and transformants were selected on SCGal −U plates. Replicas of these plates on YPD plates were subjected to cell lysis assay. From the transformants that did not show the cell lysis phenotype (see RESULTS), plasmids were recovered and then reintroduced into *sro9Δ tpm1Δ pGAL7:SRO9* cells to confirm the activity to prevent the cell lysis. Five of plasmids were isolated and the partial nucleotide sequence of these plasmids revealed that all of these plasmids carried *TPM2.*

Morphological observations: Cells grown in liquid culture ($<5 \times 10^6$ cells per ml) were harvested and stained with rhodamine-phalloidin (to reveal actin filaments), with calcofluor (to reveal cell wall chitin), or with affinity-purified rabbit anti-Sro9p antibodies (to reveal Sro9p) as the methods described (PRINGLE *et al.* 1989). For calcofluor staining, cells were stained with 2 μg/ml of calcofluor solution in 0.1 M potassium phosphate buffer (pH 7.5). For rhodamine-phalloidin staining, cells were fixed with 5% formaldehyde for 60 min, washed with phosphate-buffered saline, stained with 1:50-diluted rhodamine-phalloidin solution (Molecular Probes, Inc., Eugene, OR) for 2 hr, and washed five times with phosphate-buffered saline. For Sro9p staining, cells fixed with 5% formaldehyde for 120 min were spheroplasted, treated with 0.1 % TritonX-100 in 100 mM potassium phosphate buffer (pH 7.5) with 1 M sorbitol, and submerged in methanol (−20°) for 6 min and then in acetone (−20°) for 30 sec. Anti-Sro9p antibodies were used at a 1:2000 dilution and visualized using CY3-labeled sheep anti-rabbit IgG antibodies (Chemicon International, Inc. Temecula, CA) at a dilution of 1:50. These samples were mounted in *p*-phenylenediamine (1 mg/ml in 90% glycerol) and observed with an epifluorescencemicroscope BH-2 (Olympus, Tokyo, Japan).

To estimate the numbers of cells with or without actin cables, and the numbers of cells with polarized or depolarized actin patches, >350 cells stained with rhodamine-phalloidin were observed and counted.

Subcellular fractionation: Subcellular fractionation was performed as described by NISHIKAWA *et al.* (1990) with minor modifications. Briefly, cell extracts were prepared by disruption of spheroplasts with glass beads by vortexing in lysis buffer (10 mM triethanolamine acetate pH 7.5, 0.7 M mannitol, 0.1 M KCl and 1 mM EGTA), and the lysate was centrifuged at 150 × *g* for 5 min to remove unbroken spheroplasts. The supernatant was subjected to centrifugation at 10,000 × *g* for 10 min to yield low speed pellet (LSP) and low speed supernatant (LSS) fractions. The LSS fraction was further centrifuged at 100,000 × *g* for 60 min to yield high speed pellet (HSP) and high speed supernatant (HSS) fractions. All steps were carried out at 5°.

RESULTS

Mapping and sequence analysis of *SRO9*: High-copy number plasmids carrying *SRO9* suppressed the growth defect of *rho3Δ* cells (strain YMR505) and the temperature sensitivity of *rho3* Ts^- mutant cells (a *rho3-1* strain YMR3732-2B) at 34° (MATSUI and TOH-E 1992b, data not shown). The suppression activity was mapped to the 1.8-kb *Xho*I-*Eco*RI fragment (Figure 1A), and deter-

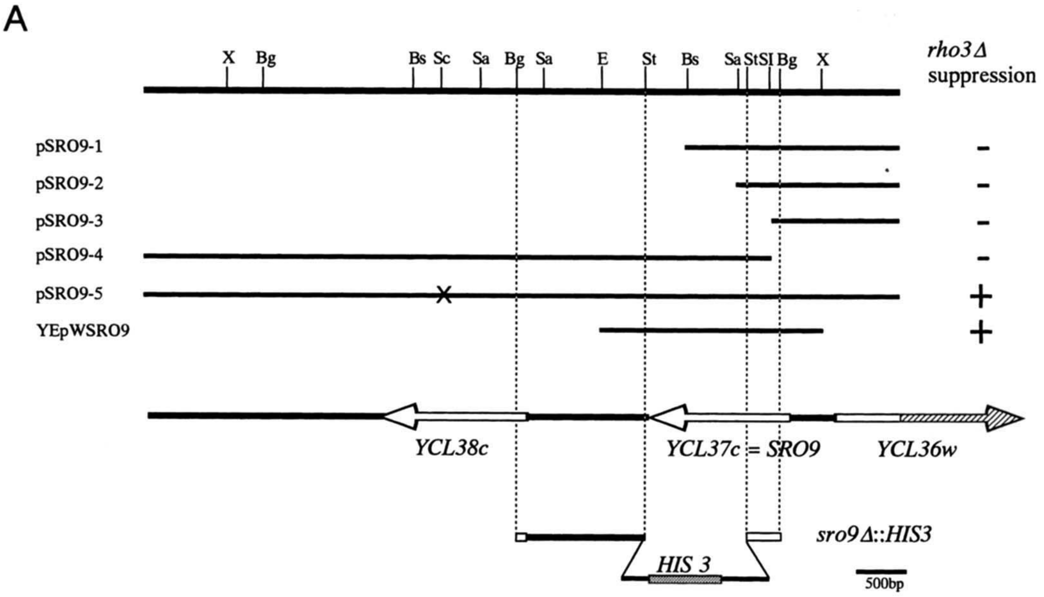

B

```
Sro9p        1:M--KIFWD-PRSVIEHQDYSGPANVFHLLFTSLPTMSA-ETAAANTATA-PVPEVQE-QE
Sro99p       1:MSSQNLNDNPKNTSSAAE-DKKKQTSSLKLAPIPTTSPWKSSSPDSNTVIPVEELRDISK
                 *     * *               *     ** *           *  ** *

Sro9p       55:SSK-SKQVNLTPAPLPTSSP-WKLAPTEIPVSTISIEDLDATRKKKNRTPTPKSSTATKW
Sro99p      60:TAKPSKNGS-GSIKL-TSNTKW--TPI-TP-S-V-I--ISGS---KD-T-NSKSGKNSKN
                  * **        * **   *   *   * *   *         *  *   **   *

Sro9p      113:VPIKASITVSGTKRSGSKNGASNGNSNKSKN-N-KTAASSTSS-SNA-NRKKKHHQHNAK
Sro99p     105:--SKTNKKM--KKR-G-KY--NNDI-NK-KDFNGQTN--STSEISNVSNLESKPLDANAK
                   *        ** * *    *   ** *  *  *   ***  **  *   *    ***

Sro9p      169:KQQQMKKDGFESAVGEEDSKDATSQENGQSTQQQQPPHHRNHHHSHHHNSNGPQRRKFHN
Sro99p     153:VNIH-SSSG-ATA--NGNIKRIT-NNN-NSTNGRQSRNYQNRNGKTRYNNN-S-RHS-QA
                     *   *      *  *   *  **   *     *        * *   *

Sro9p      229:SNNA-GMPQN-QGFPPQFKPYQGRNARNNNNNRSKY-H-NHFHHNQQHPQQP-MVKLQQQ
Sro99p     204:ANNAISFPNNYQA-RPEYIP--NASHWLNNNSRNSYKQLSYFRQQQYYNNINYQQQLQTP
                ***   * * *   *   *        *** *  *      *   *         **

Sro9p      284:-FYPVQPVLMAINNIARQIEYYFSEENLTVDNYLRSKLSK--DGFAPLSLISKFYRVVNM
Sro99p     261:YYYSMEPIFKSIESIKNQIEFYFSEENLKTDEFLRSKFKKANDGFIPMSLIGKFYRMVNL
                 *   *    *  *  *** *******  *  ****  *  *** * *** **** **

Sro9p      341:SFGGDTNLILAALREIVANEAATVNVAEGTLAAKEGDNVTGEAKEPSPLDKYFVRSKSWS
Sro99p     321:SLGGDPNLILASMREVLQHK-ET-NHLEIALGSIEGAQ-KNMADDFNPLENYFIRRENWA
               * *** *****  **        * *  *  *  **     *    **  ** *   *

Sro9p      401:NW-LPETF-----ETE-INIEKELVG-DALDQF-MISLPP-VPQQEEESSTELASQEQET
Sro99p     378:EYAMESNFDENDDETEKYNIEK-LLGPNDLDNYSYMGYPNFFPSNENGKKSQ-SYDQGEI
                       *     ***  **** * *   **        *   *  *           *

Sro9p      451:KEDSAPVAAGESESSL
Sro99p     436:SRQFEQNLQIND
```

C

```
Sro9p                    297 IAR-QIEYYFSEENLTVDNYLRSKLSK--D-GFAPLSLISKFYRV
Sro99p                   275 IKN-QIEFYFSEENLKTDEFLRSKFKKAND-GFIPMSLIGKFYRM
R144.7    (C.elegans)    523 YVRKQIEYYFSEENLQKDFFLRRKMG---PEGYLPVALIASFPRV
OSO570A   (Rice)          30 I-RTQIEFYFSTNNLCHDTFLRRQMD---DQGWVHIDVITKFNRM
LA        (Drosophila)    54 IIR-QVEYYFGDANLNRDKFLREQIGKNED-GWVPLSVLVTFKRL
Lhp1p     (S.cerevisiae)  33 CLK-QVEFYFSEFNFPYDRFLRTTAEKN-D-GWVPISTIATFNRM
LA[A]     (Xenopus)       17 ICE-QIEYYFGDHNLPRDKFLKQQI-LL-D-GWVPLETMIKFNRL
LA        (Bovine)        17 ICH-QIEYYFGDFNLPRDKFLKEQI-KL-DEGWVPLEIMIKFNRL
LA        (Human)         17 ICH-QIEYYFGDFNLPRDKFLKEQI-KL-DEGWVPLEIMIKFNRL
LA[B]     (Xenopus)       16 ICE-QIEYYFGDHNLPRDKFLKQQV-LL-DNGWVPLETMIKFNRL
LA        (Mouse)         17 ICH-QIEYYFGDFNLPRDKFLKEQI-KL-DEGWVPLETMIKFNRL
LA        (Rat)           17 ICH-QIEYYFGDFNLPRDKFLKEQI-KL-DEGWVPLETMIKFNRL
```

FIGURE 1.—(A) Map of *SRO9*. The restriction map of the *SRO9* region is shown at the top. Inserts of the plasmids are diagrammed below the map. A cross indicates the deletion created by digestion of *Sac*II followed by blunting and religation. Suppression activities to suppress the *rho3*Δ defect are summarized on the right (+ and − indicate growth and poor growth, respectively, of *rho3*Δ cells harboring the plasmids indicated on the left). Open arrows represent open reading frames, deduced from the genome sequence, in the insert of pSRO9. The construction of the disrupted allele of *SRO9* is shown diagramatically below the map. Bg, *Bgl*II; Bs, *Bst*EII; E, *Eco*RI; Sa, *Sal*I; SI, *Sac*I; Sc, *Sac*II; St, *Stu*I; X, *Xho*I. (B) Amino acid sequences of Sro9p and Sro99p. Asterisks represent the identical residues between Sro9p and Sro99p. The region conserved with the La proteins is boxed. The region that is deleted in *sro9-ΔHB* is underlined. (C) Alignment of the conserved region among Sro9p, Sro99p, and the La proteins. The residues identical with Sro9p are shaded. EMBL/GenBank/DDBJ accession numbers of the proteins are as follows: Sro9p (*YCL37c*), X59720; Sro99p (*YDR515w*), U33057; *Caenorhabditis elegans* R144.3 protein, U23515; OS0570A from a partially sequenced rice cDNA, D15392; Drosophila La protein, L32988; *S. cerevisiae* La protein homologue Lhp1p, L33023; *Xenopus laevis* La protein homologue A, X68817; bovine La protein homologue, X13698; human La protein homologue, X13697; *X. laevis* La protein homologue B, X68818; mouse La protein homologue, L00993; and rat La protein homologue, X67859.

mination of its nucleotide sequence revealed that the fragment carried *YCL37c* (OLIVER *et al.* 1992) on chromosome III. *YCL37c* is the only open reading frame in the 1.8-kb *XhoI-EcoRI* region that was sufficient for suppressing the *rho3Δ* defect (Figure 1A), indicating that *SRO9* is *YCL37c*. *SRO9* encodes a hydrophilic protein of 466 amino acids, deduced from a hydrophathy plot (KYTE and DOOLITTLE 1982). A homology search using the FASTA program against the EMBL database revealed that Sro9p possesses a domain homologous to one conserved among the La proteins (YOO and WOLIN 1994) and that yeast possesses a gene (*YDR515w*) highly related to *SRO9* (Figure 1, B and C). The protein encoded by *YDR515w* is 33.6% identical to Sro9p (Figure 1B). We have designated the gene (*YDR515w*) as *SRO99*, since it is related to *SRO9* both structurally and functionally (see below). The La protein belongs to the RNA recognition motif superfamily of RNA-binding proteins (KENAN *et al.* 1991). The La protein possesses the RNA recognition motifs and a domain promoting homodimerization of the La protein; however, the domain, conserved between *SRO9* and the La protein, is distinct from those (CRAIG *et al.* 1997; YOO and WOLIN 1994).

Gene disruption of *SRO9*: To characterize Sro9p function, we disrupted *SRO9* in diploid strain YPH501, and heterozygous diploids were sporulated and dissected. From each tetrad, we obtained four viable spore clones. The *sro9Δ::HIS3* segregants were indistinguishable from wild-type segregants in growth rate and in morphology at 15, 25, 30, and 37°. In addition, the budding pattern, actin organization, osmotic sensitivity (as judged by growth on YPD containing 1 M sorbitol), and mating efficiency of the *sro9Δ::HIS3* segregants were indistinguishable from wild-type segregants. Therefore, we conclude that Sro9p is not essential for the phenotypes we observed.

It might be possible that the gene highly related to *SRO9* (*SRO99*, Figure 1B) is redundant with *SRO9*. To examine this possibility, we disrupted *SRO99* in a diploid strain YPH501 and heterozygous diploid cells were sporulated and dissected. From each tetrad, we obtained four viable spore clones and all segregants grew well at 15, 25, 30, and 37°, indicating that *SRO99* is dispensable for growth. We mated the *sro99Δ::URA3* segregants (strain YMK013) to an *sro9Δ::HIS3* strain (YMK011A) and the resultant diploid cells were sporulated and dissected. His$^+$ Ura$^+$ segregants (*sro9Δ::HIS3 sro99Δ::URA3* segregants) grew as well as wild-type segregants at 15, 25, 30, and 37° and displayed the budding pattern and actin distribution that were indistinguishable from those of the wild-type segregants (data not shown). From these results, we concluded that Sro9p and Sro99p are not essential for vegetative growth and the phenotypes that we observed.

Genetic interactions between *SRO9* and *TPM1*: The phenotypes of *rho3* mutant cells and the genetic interactions of *RHO3* with *BEM1* and *SEC4* suggest that Rho3p function is involved in proper organization of the actin cytoskeleton and in vectorial transport of secretory vesicles (MATSUI and TOH-E 1992b; IMAI *et al.* 1996). To examine whether Sro9p also participated in these processes, we tested synthetic lethal interactions of *SRO9* with the genes related to these processes, such as *MYO1* for a conventional myosin, *MYO2* for an unconventional myosin of the myosin I family, *TPM1, SEC4, BEM1, CDC42,* and *RHO3*. Each of *myo1Δ::LEU2* cells (strain YMK024), *myo2-66* mutant cells (strain YMK021), *tpm1Δ::URA3* cells (strain YMK014), *sec4-2* mutant cells (strain YJS4-2A), *bem1Δ::URA3* cells (strain YMK007), *cdc42-1* cells (strain YMR420), and *rho3-1* cells (strain YMR3732-2B) were mated to *sro9Δ::HIS3* cells (strain YMK011A or YMK011B). The resultant diploid cells were sporulated and dissected.

Except for the tetrads derived from either *sro9Δ/+ rho3-1/+* diploid cells or *sro9Δ/+ tpm1Δ/+* diploid cells, almost all of the tetrads produced four viable spore clones, including double mutant segregants. *myo1Δ::LEU2 sro9Δ::HIS3* segregants and *bem1Δ::URA3 sro9Δ::HIS3* segregants grew as well as *myo1Δ::LEU2* and *bem1Δ::URA3* segregants, respectively, and the temperature sensitivities were indistinguishable between *sec4-2* segregants and *sec4-2 sro9Δ::HIS3* segregants, between *myo2-66* segregants and *myo2-66 sro9Δ::HIS3* segregants, and between *cdc42-1* segregants and *cdc42-1 sro9Δ::HIS3* segregants, indicating that *sro9Δ::HIS3* is not synthetic-lethal with these mutations. In case of *rho3-1*, a temperature-sensitive mutant allele of *RHO3*, *rho3-1 sro9Δ::HIS3* segregants formed microcolonies and grew much more poorly than *rho3-1 SRO9*$^+$ segregants, indicating a synthetic defect of *sro9Δ* with *rho3-1*.

Strikingly, in the case of *tpm1Δ*, we did not obtain any *tpm1Δ::URA3 sro9Δ::HIS3* segregant at 25° from *tpm1Δ::URA3/+ sro9Δ::HIS3/+* heterozygous diploid cells, suggesting a synthetic-lethal interaction between *SRO9* and *TPM1*. To confirm this interaction, *tpm1Δ::URA3/+ sro9Δ::HIS3/sro9Δ::HIS3* diploid cells (strain YMK012) were subjected to tetrad analysis. Out of 63 tetrads dissected, at 25°, 59 tetrads produced two viable and two inviable segregants, and four tetrads produced two viable segregants, one segregant that formed a microcolony on a dissection slab but could not propagate further, and one inviable segregant. All healthy viable segregants were Ura$^-$, indicating that the combination of *sro9Δ* with *tpm1Δ* is lethal.

For further characterization of the genetic interaction between *SRO9* and *TPM1*, additional copies of *SRO9* were introduced into *tpm1Δ* cells. Disruption of *TPM1* results in reducing the growth rate, inability to grow at 37°, and the disappearance of actin cables (LIU and BRETSCHER 1989, 1992). The temperature sensitivity of *tpm1Δ* cells was not suppressed by a high dose of *SRO9* (data not shown). However, the doubling time in YPD medium at 25° of *tpm1Δ* cells (strain YMK017)

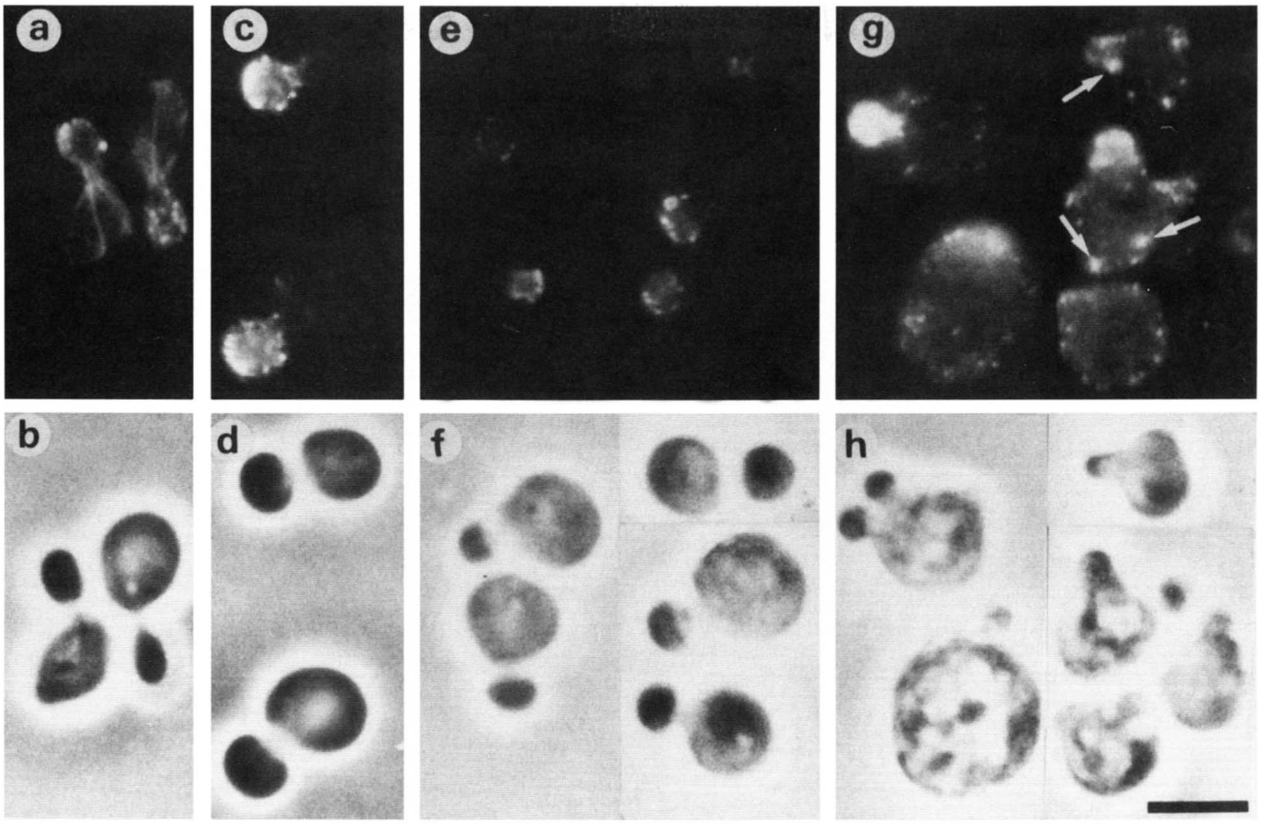

FIGURE 2.—Effect of Sro9p on morphology of *tpm1Δ* cells and *sro9Δ tpm1Δ* cells. *tpm1Δ* cells carrying *pGAL7:SRO9* (strain YMK017) (a–d) were grown in YPGal (a and b) or YPD (c and d). *sro9Δ tpm1Δ* cells carrying *pGAL7:SRO9* cells (strain YMK018) (e–h) were grown in YPGal, shifted to YPD, harvested 0 (e and f) or 24 hr (g and h) after the shift. Cells were stained with rhodamine-phalloidin to reveal actin (a, c, e, and g). (b, d, f, and h) Phase-contrast images. Arrows indicate abnormal clusters of actin patches. Yeast cells were cultured at 25°. Bar, 5 μm.

with YEpWSRO9, a high-copy number plasmid carrying *SRO9*, was 133 ± 3 min, whereas that of *tpm1Δ* cells carrying a control plasmid (YEplac112) was 160 ± 7 min. These results indicate that a high dose of *SRO9* suppresses the reduced growth rate of *tpm1Δ* cells.

We also constructed *tpm1Δ* cells with integrated *pGAL7:SRO9*, *SRO9* under the control of a galactose-dependent promoter. When induced, *pGAL7:SRO9* produced almost an equivalent amount of Sro9p to that from the original *SRO9* allele, as estimated from Western analysis using anti-Sro9p sera, and suppressed the reduced growth rate of *tpm1Δ* cells (data not shown). To examine the effect of Sro9p on actin cytoskeleton in *tpm1Δ* cells, actin filaments in *tpm1Δ* cells bearing *pGAL7:SRO9* was stained with rhodamine-phalloidin. About 84% of *tpm1Δ* cells expressing *pGAL7:SRO9* restored actin cables (Figure 2a), whereas >96% of *tpm1Δ* cells without expression of *pGAL7:SRO9* did not possess observable actin cables (Figure 2c). These results indicate that overexpression of *SRO9* suppresses the disappearance of actin cables in *tpm1Δ* cells.

The phenotypes of Sro9p-depleted *tpm1Δ* cells: To explore further the function of Sro9p in a *tpm1Δ* background, an *sro9Δ tpm1Δ* strain carrying *pGAL7:SRO9* (strain YMK018) was constructed. The *sro9Δ tpm1Δ pGAL7:SRO9* cells grew on YPGal (data not shown), but their growth was arrested 16 hr after a shift to YPD (Figure 3A). In galactose-containing medium, the *sro9Δ tpm1Δ pGAL7:SRO9* cells produced almost an equivalent amount of Sro9p to that in wild-type cells (data not shown), showed a normal cell shape (Figure 2f), and had actin patches concentrated in the bud (Figure 2e). These phenotypes were similar to those observed in *tpm1Δ* cells (Figure 2, c and d). In contrast, all of the *sro9Δ tpm1Δ pGAL7:SRO9* cells that were arrested by the depletion of Sro9p became enlarged and rounded, or acquired an aberrant shape (Figure 2h), and cell lysis was detected (Figure 3B). In these cells, actin patches were scattered over the cell surface (Figure 2g) and abnormal clusters of the patches were observed (indicated by arrows in Figure 2g). These results suggest that *SRO9* is required for proper organization of the actin cytoskeleton in *tpm1Δ* cells.

The domain conserved between Sro9p and the La proteins is essential for Sro9p function: Using the synthetic-lethality of *sro9Δ* with *tpm1Δ*, we examined whether the domain conserved between Sro9p and the La proteins (Figure 1C) was important for Sro9p function. We constructed a truncated version of *SRO9*, *sro9-ΔHB*, in which the region for the conserved domain

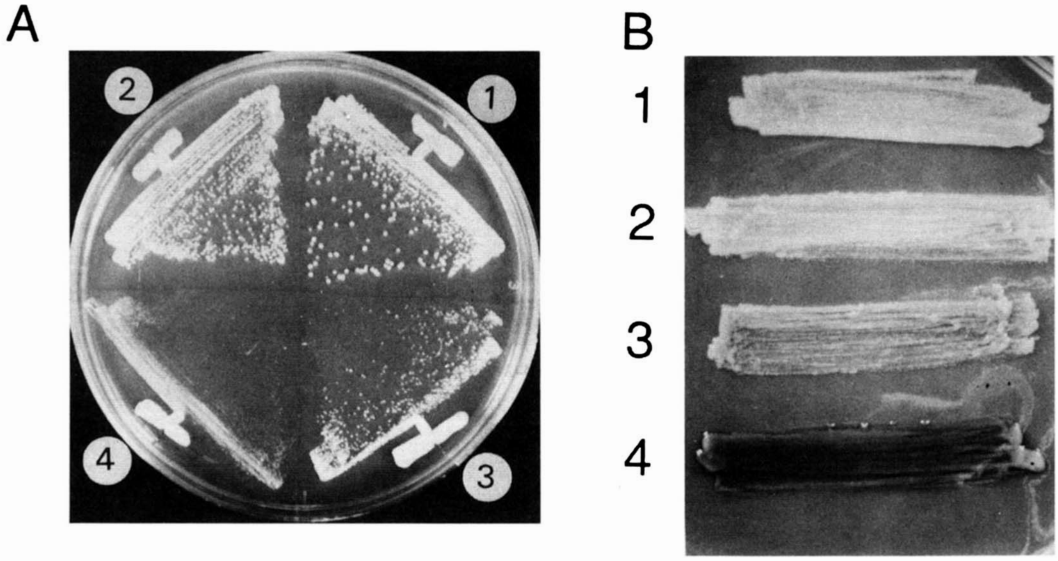

FIGURE 3.—Depletion of Sro9p in *tpm1*Δ cells. (1) Wild-type cells carrying *pGAL7:SRO9* (strain YMK016), (2) *sro9*Δ cells carrying *pGAL7:SRO9* (strain YMK019), (3) *tpm1*Δ cells carrying *pGAL7:SRO9* (strain YMK017), and (4) *sro9*Δ *tpm1*Δ cells carrying *pGAL7:SRO9* (strain YMK018) were streaked on YPD plates and incubated at 25° for 2 days (A) and overlaid with BCIP solution (B). Black regions in the photograph in B were blue, indicating cell lysis.

was truncated (Figure 1B). The introduction of *sro9-ΔHB* either on a low copy-number plasmid (pRS316-SRO9ΔHB) or on a high copy-number plasmid (YEplac195-SRO9ΔHB) did not suppress the growth defect of *sro9*Δ *tpm1*Δ *pGAL7:SRO9* cells (strain YMK018-1) in YPD (data not shown). The amount of the truncated Sro9p produced from pRS316-SRO9ΔHB was almost equivalent to that of the intact Sro9p in wild-type cells, as estimated by Western analysis (data not shown). These results suggest that the truncated region, which overlaps with the domain conserved between Sro9p and the La proteins, plays an important role in the Sro9p function.

***TPM1* suppresses the growth defect of *rho3*Δ cells:** The strong genetic interactions between *SRO9* and *TPM1* raised the possibility that *TPM1,* when overexpressed, could suppress the *rho3*Δ defect. A high-copy number plasmid, carrying *TPM1* under the control of the *GAL1* promoter, produces a significant amount of Tpm1p even in glucose-containing medium (LIU and BRETSCHER 1989). We introduced this plasmid into *rho3*Δ cells (strain YMR505) and temperature-sensitive *rho3* mutant cells (a *rho3-1* strain YMR3732-2B). *rho3*Δ cells carrying this plasmid grew well, whereas *rho3*Δ cells without this plasmid grew very poorly (Figure 4A). *rho3-1* cells with this plasmid could grow at 34° but *rho3-1* cells without the plasmid did not (data not shown). These results indicate that the overexpression of *TPM1* suppresses the *rho3* defect.

In *rho3*Δ cells, actin patches were delocalized and actin cables disappeared. Most (~76%) of the *rho3*Δ cells with a control plasmid, YEp24, still had delocalized actin patches and no observable actin cables, and the rest had delocalized actin patches and actin cables observed very faintly (Figure 4B-a). In contrast, ~56% of *rho3*Δ cells overexpressing *TPM1* and ~57% of *rho3*Δ cells overexpressing *SRO9* possessed networks of actin cables and cortical actin patches that were localized properly in the bud (Figure 4B, c and e). These results suggest that overproduction of Tpm1p, as well as that of Sro9p, suppresses the defect in organization of actin cytoskeleton in *rho3*Δ cells.

***TPM2* was isolated as a multicopy suppressor of the synthetic defect of *tpm1*Δ with *sro9*Δ:** To elucidate the role of Sro9p and Tpm1p in vegetative growth, we screened for genes whose overexpression could suppress the lysis phenotype of Sro9p-depleted *tpm1*Δ cells (Figure 3B). Five plasmids were isolated as multicopy suppressors of the lysis phenotype and all of these plasmids carried *TPM2.* The activity to suppress the cell lysis phenotype was mapped in *TPM2* (data not shown). The growth defect of *tpm1*Δ *sro9*Δ cells also was suppressed by overexpression of *TPM2* (Figure 5, sectors 3 and 4). In addition, overexpression of *TPM2* suppressed the reduced growth rate of *tpm1*Δ cells (Figure 5, sectors 1 and 2): the doubling time in the YPD medium at 25° of *tpm1*Δ cells (strain YMK017-1) carrying *TPM2* on a high-copy number plasmid (YEpUTPM2) was 98 ± 8 min, whereas that of *tpm1*Δ cells carrying a control plasmid (YEplac195) was 160 ± 7 min. Therefore, we conclude that overexpression of *TPM2* suppresses the lysis phenotype and growth defect of *tpm1*Δ *sro9*Δ cells by compensating for *TPM1* function. These results, along with the structural property and biochemical property of Tpm2p (DREES *et al.* 1995), indicate that Tpm2p is functionally redundant to Tpm1p.

DREES *et al.* (1995) have reported that disruption of *TPM2* does not affect cell growth (as also observed in Figure 6A sector 2) and that the simultaneous disruption of *TPM1* and *TPM2* is lethal. To test whether tropomyosin functions were essential in our strain background, *tpm2*Δ cells were mated to *tpm1*Δ cells and the resultant diploid cells were subjected to tetrad analysis. Among 12 tetrads, we obtained eight *tpm1*Δ *tpm2*Δ segregants at 25°. *tpm1*Δ *tpm2*Δ cells grew much more slowly than *tpm1*Δ cells at 25° (Figure 6A) and were

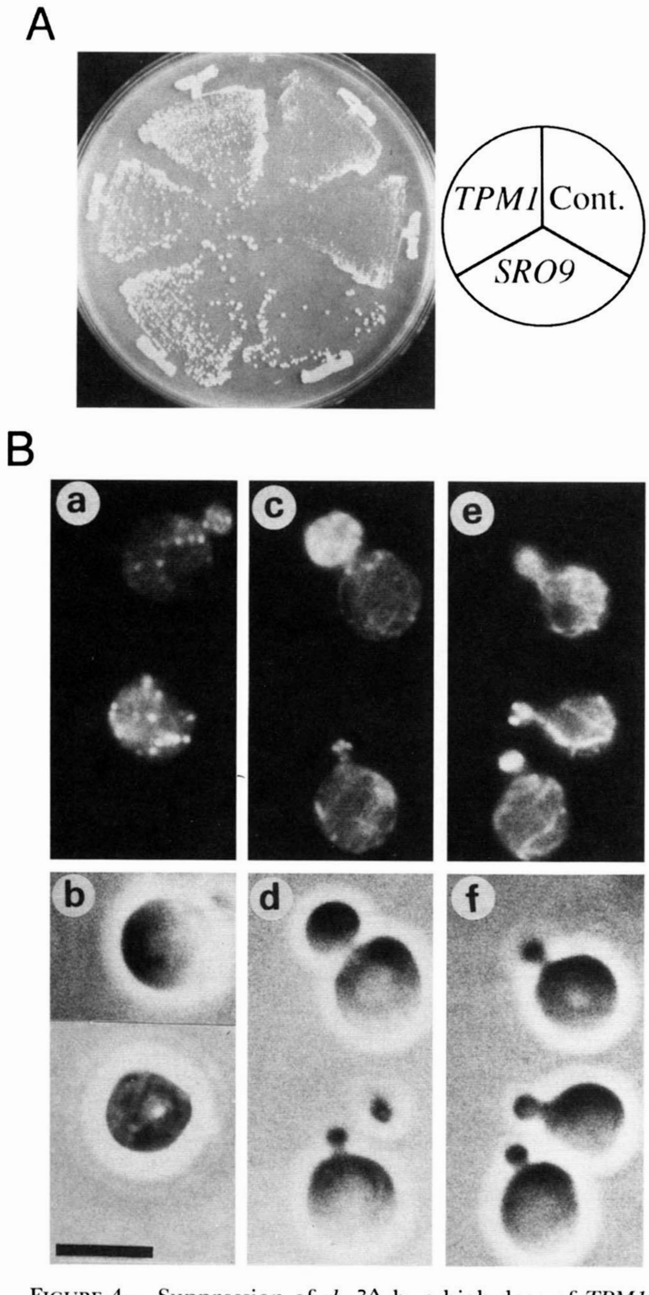

FIGURE 4.—Suppression of *rho3*Δ by a high dose of *TPM1* and *SRO9*. (A) *rho3*Δ cells (strain YMR505) with YEp24, pSRO9, or a *TPM1* overexpression plasmid (LIU and BRETSCHER 1989) were streaked on a SC −U plate and incubated at 30° for 3 days. (B) *rho3*Δ cells (strain YMR505) with YEp24 (a and b), pSRO9 (c and d), and the *TPM1* overexpression plasmid (e and f) were grown in SC −U at 30°. Cells were harvested and stained with rhodamine-phalloidin to reveal actin (a, c and e). (b, d and f) Phase-contrast images. Bar, 5 μm.

inviable at 37° (data not shown). Since *TPM1* and *TPM2* are the only genes encoding tropomyosin in *S. cerevisiae*, these results indicate that tropomyosin function is important but not essential, at least, in the genetic background of the strains used in these studies.

***SRO9* suppresses the growth defect of the cells lacking tropomyosin:** To test whether overexpression of

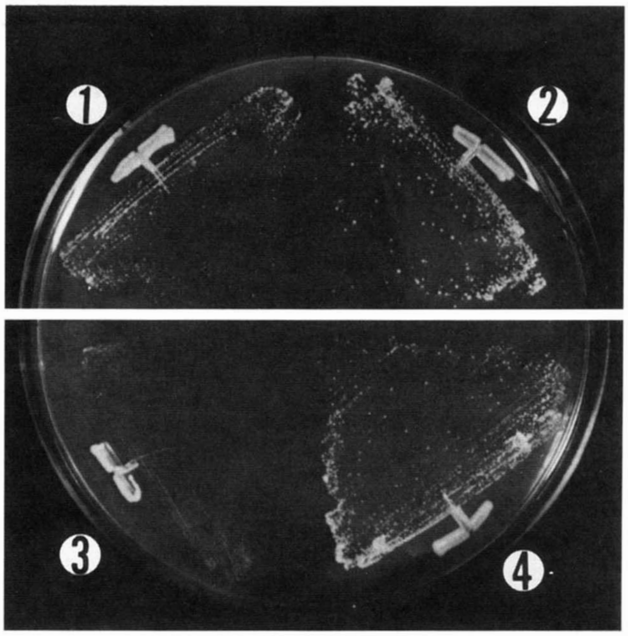

FIGURE 5.—Suppression of *tpm1*Δ by a high dose of *TPM2*. *tpm1*Δ cells (strain YMK017-1) (1 and 2) and *sro9*Δ *tpm1*Δ cells (strain YMK018-1) (3 and 4) were transformed with YEp24 (1 and 3) or YEpUTPM2 (2 and 4) on SCGal −U plates and were streaked on a SC −U plate and incubated at 25° for 2 days. More than five of independent transformants with each plasmid were tested and the results were essentially identical to that shown in the figure.

SRO9 could suppress the complete loss of the tropomyosin function, we introduced YEpWSRO9 into *tpm1*Δ *tpm2*Δ cells (strain YMK020-4B). The *tpm1*Δ *tpm2*Δ cells bearing YEpWSRO9 grew much better than those bearing YEplac112 (Figure 6B, sectors 1 and 2). In *tpm1*Δ *tpm2*Δ cells with YEplac112, actin cables disappeared (100% of the cells) and the majority of the cells (~74%) displayed delocalization of the actin patches (Figure 6C-a). In contrast, in *tpm1*Δ *tpm2*Δ cells with YEpWSRO9, although actin cables were still invisible, ~58% of the cells possessed polarized actin patches that were localized exclusively at the bud (Figure 6C-c). These results suggest that complete loss of the tropomyosin function abolishes the polarized distribution of cortical actin patches and the defect is suppressed by Sro9p.

***SRO99* can serve as a multicopy suppressor of the tropomyosin defect:** We tested whether *SRO99* also could serve as a multicopy suppressor of the tropomyosin defect. *tpm1*Δ *tpm2*Δ cells with YEpWSRO99, a multicopy plasmid carrying *SRO99*, grew better than the *tpm1*Δ *tpm2*Δ cells without the plasmid (Figure 6B, sectors 1 and 3). Although actin cables were not visible, ~58% of the *tpm1*Δ *tpm2*Δ cells with YEpWSRO99 displayed polarized localization of actin patches. Without the plasmid, only 26% of *tpm1*Δ *tpm2*Δ cells displayed polarized actin patches. These results indicate that *SRO99* can serve as a multicopy suppressor of the tropomyosin defect. Although introduction of YEpWSRO99

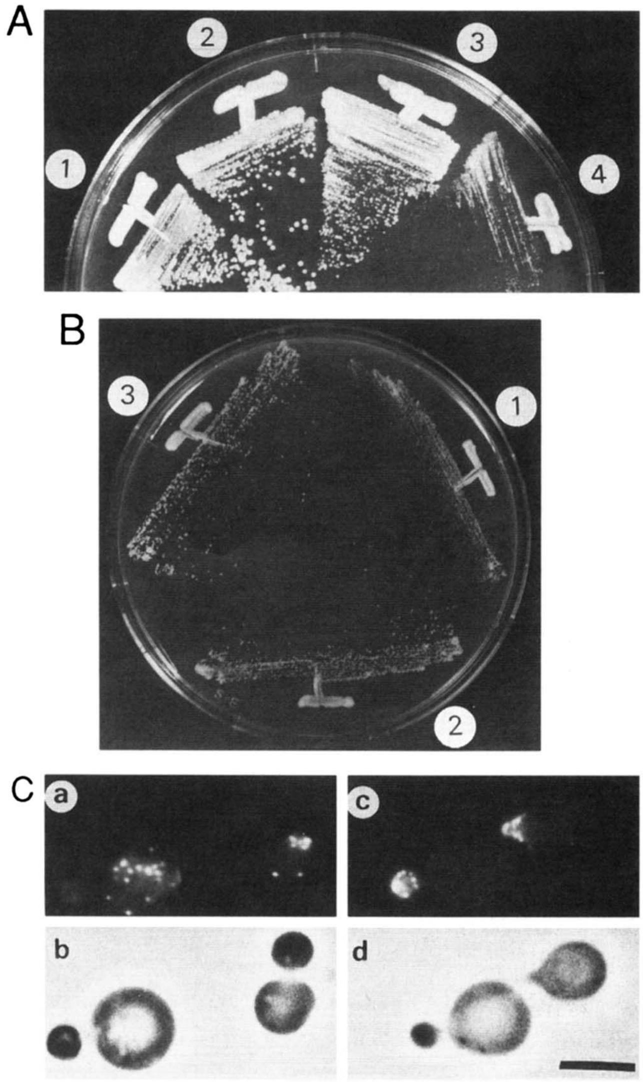

FIGURE 6.—Phenotypes of *tpm1Δ tpm2Δ* cells. (A) The siblings derived from a *tpm1Δ/+ tpm2Δ/+* diploid cell (strain YMK020) [wild-type segregant (YMK020-4A) (1), *tpm2Δ* segregant (YMK020-4C) (2), *tpm1Δ* segregant (YMK020-4D) (3), and *tpm1Δ tpm2Δ* segregant (YMK020-4B) (4)] were streaked on a YPD plate and incubated at 25° for 2 days. (B) *tpm1Δ tpm2Δ* cells (strain YMK020-4B) were transformed with YEplac112 (1), YEpWSRO9 (2), or YEpWSRO99 (3), and the transformants were streaked on a SC −W plate and incubated at 25° for 2 days. More than five of independent transformants with each plasmid were tested and the results were essentially identical to that shown in the figure. (C) Morphology of *tpm1Δ tpm2Δ* cells. *tpm1Δ tpm2Δ* cells (strain YMK020-4B) with YEplac112 (a and b) or YEpWSRO9 (c and d) were grown in SC −W at 25°. Cells were harvested and stained with rhodamine-phalloidin to reveal actin (a and c). (b and d) Phase-contrast images. Bar, 5 μm.

failed to suppress the *rho3Δ* defect (data not shown), from the similarity between *SRO9* and *SRO99* on the structure of their gene products and the similar ability to suppress the tropomyosin defect, we concluded that *SRO99* is functionally redundant with *SRO9*.

It is unclear why a high dose of *SRO99* did not suppress the *rho3Δ* defect. However, in *tpm1Δ* cells, disruption of *SRO9* was lethal but that of *SRO99* was not (data not shown), suggesting that *SRO99* functions less well than *SRO9*. Therefore, it is possible that the expression of *SRO99* on a high-copy number plasmid is not sufficient to suppress the *rho3Δ* defect, although the expression of *SRO9* on a high-copy number plasmid can.

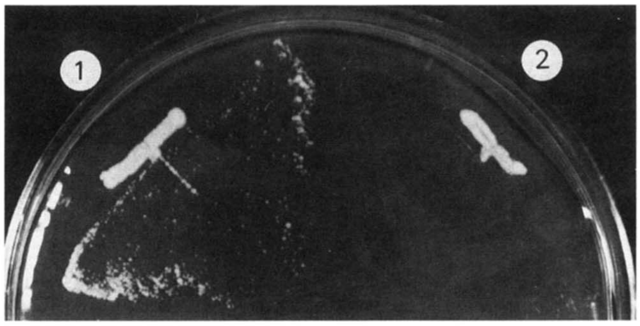

FIGURE 7.—Suppression of *act1-1* defect by a high dose of *SRO9*. *act1-1* cells (strain YMK022) with YEpWSRO9 (1) or YEplac112, a control plasmid (2), were streaked on SC −W plate and incubated at 36° for 2 days. More than five of independent transformants with each plasmid were tested and the results were essentially identical to that shown in the figure.

Overexpression of *SRO9* suppresses the *act1-1* defect: Along with the genetic interactions between *SRO9* and tropomyosin genes, overproduction of Sro9p can restore actin cables in *tpm1Δ* cells and in *rho3Δ* cells. These results suggest that Sro9p plays a role in organization of the actin cytoskeleton. To test the genetic interaction between *ACT1* and *SRO9*, we introduced *SRO9* on a high-copy number plasmid into *act1* mutant cells. Actin filaments in *act1-1* mutant cells are unstable and *act1-1* cells exhibit temperature-sensitive growth, disappearance of actin cables, and delocalization of actin patches (NOVICK and BOTSTEIN 1985). At 36° *act1-1* cells with a control plasmid grew very poorly, but *act1-1* cells overexpressing *SRO9* grew much better (Figure 7), indicating that *SRO9* can serve as a multicopy suppressor of *act1-1*. In *act1-1* cells, even at 25°, few actin cables were seen and the actin patches were delocalized (NOVICK and BOTSTEIN 1985, data not shown). In *act1-1* cells overexpressing *SRO9*, although actin cables were still invisible, actin patches were localized at the bud at 25° (data not shown). The suppression of *act1* defect with *SRO9* is allele-specific since overexpression of *SRO9* did not suppress the temperature sensitivity caused by *act1-2* (strain YMK023), another temperature-sensitive allele of *ACT1* (data not shown).

We introduced a plasmid overproducing Tpm1p (LIU and BRETSCHER 1989) to examine whether overexpression of *TPM1* could suppress the temperature sensitivity of *act1* mutant cells. Introduction of the plasmid did not suppress the temperature sensitivity of both *act1-2* (data not shown; LIU and BRETSCHER 1989) and *act1-1* at 35° (data not shown).

Subcellular localization of Sro9p: We determined the localization of Sro9p by subcellular fractionation

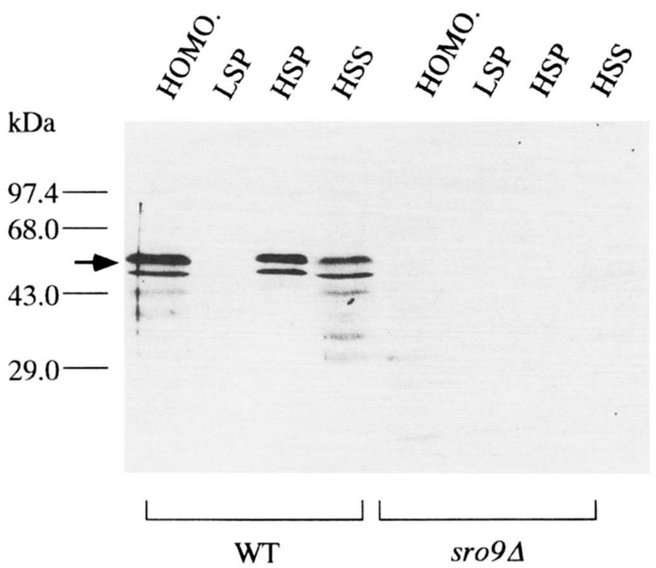

FIGURE 8.—Subcellular fractionation of Sro9p. Each of the fractions (HOMO, total extract; LSP; HSP; and HSS) from ~6.4×10^5 cells (WT, wild-type strain YPH500; *sro9*Δ, *sro9*Δ strain YMK011B) was fractionated by 10% SDS-polyacrylamide gel electrophoresis and analyzed by Western blotting using anti-Sro9p antibodies. The migration positions of molecular weight markers are shown at the left. An arrow indicates the migration position of Sro9p.

and by immunofluorescence-microscopy. Extracts of isogenic wild-type or *sro9*Δ cells were fractionated into LSP (low speed pellet; containing plasma membrane components as well as other dense materials), HSP (high speed pellet; containing high dense materials such as a large protein complex), and HSS (high speed supernatant; containing soluble proteins that are diffused in cytoplasm) fractions. Western analysis of these fractions using anti-Sro9p polyclonal antibodies revealed that Sro9p was fractionated in the HSS and HSP fractions of wild-type cells (Figure 8). Sro9p was not fractionated in LSP fractions, suggesting that the Sro9p did not associate with the membranes. Indirect immunofluorescence-microscopic analysis using the anti-Sro9 antibodies revealed that Sro9p was detected as dots in the cytoplasm throughout the cell cycle (Figure 9).

DISCUSSION

Tpm1p and Tpm2p are functionally equivalent and tropomyosin is not essential in yeast: From the complete yeast genome sequence, yeast has only two genes for tropomyosin (*TPM1* and *TPM2*). It has been reported that *TPM1* and *TPM2* play distinct roles in cell growth in spite of the similarity of the structural and biochemical properties, mainly because *TPM2* fails to serve as a multicopy suppressor of *tpm1*Δ (DREES *et al.* 1995). In the previous report, they used a plasmid carrying *TPM2* under the control of the *GAL1* promoter for examining suppression. We also failed to detect suppression of *tpm1*Δ with this plasmid (data not shown). However, in this study, we have found that *TPM2* can serve as a multicopy suppressor of *tpm1*Δ when *TPM2* is on a high-copy-number plasmid (Figure 5). Since overexpression of *TPM2* with the *GAL1* promoter did not inhibit cell growth (DREES *et al.* 1995, data not shown), it is unlikely that expression of *TPM2* with the *GAL1* promoter itself has a toxic effect that inhibits the suppression. It remains unclear why expression of *TPM2* under control of the *GAL1* promoter did not suppress the *tpm1*Δ defect. However, the fact that *TPM2* can serve as a multicopy suppressor of *tpm1*Δ, along with the similarity of the structural and biochemical properties (DREES *et al.* 1995), suggests that *TPM1* and *TPM2* are functionally equivalent. However, the effect of the gene disruption on cell growth is different between *TPM1* and *TPM2*: *tpm1*Δ cells grow poorly but *tpm2*Δ cells grow well (DREES *et al.* 1995, Figure 6A). These facts indicate that *TPM1* plays a more major role in tropomyosin function.

In a previous article *tpm1*Δ *tpm2*Δ cells were reported to be lethal (DREES *et al.* 1995). However, in our study *tpm1*Δ *tpm2*Δ cells were viable, but grew very slowly (Figure 6A). It is not a rare for a growth defect to vary in different genetic backgrounds. The phenotype caused by the loss of a factor involved in bud emergence has been previously observed to vary with genetic background, *e.g.*, the restrictive temperature for deletion of either *BEM1*, *BEM2*, or *BEM4* can vary from one strain to another (MACK *et al.* 1996). It is plausible that the genetic background of the strains used in the previous article is more sensitive to the loss of tropomyosin genes than is our strain background. From the genetic evidence shown in this study, we conclude that *TPM1* and *TPM2* are functionally redundant and, at least in the genetic background used in this article, tropomyosin function is important but not essential for vegetative cell growth.

Sro9p functions like Tpm1p: Since the disruption of tropomyosin is not lethal, it is possible that some factor(s) compensates for the loss of tropomyosin function, stabilizing actin filaments and undergoing transport of membrane vesicles for cell growth. Sro9p is a strong candidate for this function, since (1) overexpression of *SRO9* can suppress the total loss of tropomyosin (Figure 6B), (2) overexpression of *SRO9* restores actin cables in *tpm1*Δ cells (Figure 2a), (3) *tpm1*Δ is synthetically lethal with *sro9*Δ, and (4) Sro9p prevents *tpm1*Δ cells from undergoing cell lysis (Figure 3B). In addition to these observations, *TPM1* and *SRO9* show similar effects on *rho3*Δ cells, such that both *TPM1* and *SRO9* can serve as a multicopy suppressor of *rho3*Δ (Figure 4A), and both overexpression of *TPM1* and overexpression of *SRO9* can restore actin cables in *rho3*Δ cells (Figure 4B). Since Sro9p suppressed the growth defect of simultaneous disruption of *TPM1* and *TPM2*, it is unlikely that Sro9p affects stability of actin filaments via tropomyosin. Although computer analysis

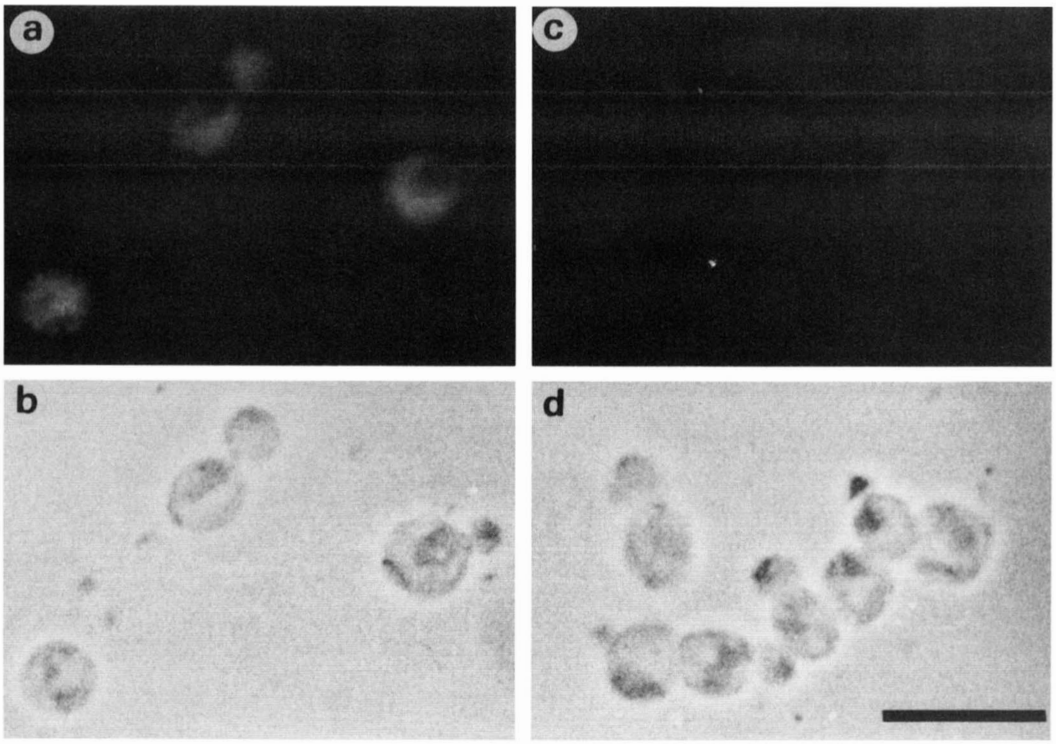

FIGURE 9.—Immunofluorescent staining of Sro9p. Wild-type cells (strain YPH501) (a and b) and *sro9*Δ cells (strain YMK011C) (c and d) were grown in YPD at 25°. Cells were fixed and prepared for indirect immunofluorescence using anti-Sro9p antibodies as described in MATERIALS AND METHODS. (b and d) Phase-contrast images. (a and c) Fluorescence microscopy. Bar, 10 μm.

did not detect any significant homology between Sro9p and tropomyosin, these results might suggest that Sro9p has an activity similar to tropomyosin. However, Tpm1p is associated with actin cables (LIU and BRETSCHER 1989; DREES *et al.* 1995), but Sro9p is not (Figures 8 and 9). In addition, we failed to detect any ability of Sro9p to bind actin using a co-sedimentation assay with rabbit actin and bacterially produced GST-Sro9p (data not shown). Altogether, it is unlikely that Sro9p possesses biochemical properties similar to those of tropomyosin.

We detected Sro9p as dots in cytoplasm using indirect immunofluorescence-microscopic analysis. Using sucrose-gradient sedimentation analysis, Sro9p in cell extracts was found in fractions containing molecules of higher molecular weights than that of Sro9p (M. KAGAMI, A. TOH-E and Y. MATSUI, unpublished results). It may be possible that Sro9p is in a protein complex that stains as dots in the cytoplasm.

Tropomyosin and Sro9p are involved in the proper organization of actin cytoskeleton: The Rho3p GTPase is required to maintain the cell polarity that controls localization of cortical actin patches and then the positions of surface growth (IMAI *et al.* 1996). *CDC42* and *BEM1,* which are required for establishing cell polarity, and *SEC4,* which is essential for the fusion of secretory vesicle to plasma membrane and thus contributing surface growth, were identified as multicopy suppressors of *rho3*Δ (MATSUI and TOH-E 1992b; IMAI *et al.* 1996). Since both *SRO9* and *TPM1* can serve as multicopy suppressors of *rho3*Δ, it might be possible that *SRO9* and *TPM1* participate in maintaining cell polarity and in surface growth. We found that asymmetric distribution of actin cytoskeleton was disrupted in *tpm1*Δ *tpm2*Δ cells (Figure 6C-a) and *tpm1*Δ *sro9*Δ cells (Figure 2g) and that *tpm1*Δ *sro9*Δ cells lysed (Figure 3B). These phenotypes suggest that Sro9p and tropomyosin play a role in maintaining polarized organization of actin cytoskeleton and in extension of cell surface.

Sro9p may stabilize actin filaments in actin cables: Sro9p can serve as a multicopy suppressor of the defects in the stability of actin filaments due to a loss of tropomyosin or the *act1-1* mutation. The suppression of the *act1* defect by *SRO9* is allele-specific since overexpression of *SRO9* could suppress *act1-1* but did not suppress *act1-2* (data not shown). *act1-1* mutant cells have a defect in the stability of actin filaments, causing temperature sensitivity (NOVICK and BOTSTEIN 1985). In contrast, actin in *act1-2* cells has some defect in transition from G-actin to F-actin rather than in stability of actin filaments, since some *act1-2* cells have an actin bar, which is an actin-aggregate that is insensitive to phalloidin (NOVICK and BOTSTEIN 1985). The allele-specific suppression suggests that Sro9p can stabilize unstable actin filaments.

Although we have failed to detect actin-binding activity of Sro9p (data not shown), we cannot exclude the possibility that Sro9p has a weak activity to bind actin. Most of actin binding proteins so far studied were identified using biochemical methods, based on their ability to bind to actin. This may be because proteins that strongly bind to actin are much more accessible for study than proteins that weakly bind to actin. However, by genetic approaches, it should be possible to identify genes that encode proteins that bind actin, but not strongly enough to be detected by biochemical methods. The genetic analysis of *SRO9* in this article suggests that Sro9p may be such a protein. The strong genetic interactions of *SRO9* with *TPM1* and with *ACT1* suggest that Sro9p function overlaps or is related to tropomyosin function, *i.e.*, the function for stabilizing actin cables. It may be possible that Sro9p acts in the cytoplasm as a factor for accelerating the polymerization of actin for actin cables and/or for inhibiting the dissociation of actin from actin cables.

Concerning actin patches, abnormal clusters of actin patches were observed in *tpm1Δ* cells when Sro9p was depleted (Figure 2g). This suggests that Sro9p may function to control the formation or localization of actin patches.

The Rho3p GTPase is involved in directing the location of actin patches and then the location for surface growth (IMAI *et al.* 1996). Since both Sro9p and Tpm1p play roles in organizing proper actin cytoskeleton, the fact that both *SRO9* and *TPM1* can serve as multicopy suppressors of *rho3Δ* is consistent with the hypothesis that Sro9p and tropomyosin act downstream of Rho3p to stabilize the polarized actin cytoskeleton that mediates surface growth.

The domain conserved among the La protein, Sro9p, and Sro99p: Sro9p and Sro99p both have a domain conserved among the La proteins (Figure 1C). Both *SRO9* and *SRO99* can serve as a multicopy suppressor of the tropomyosin defect (Figure 6B). The deletion of the La homology region of Sro9p (see Figure 1B) abolished the ability of Sro9p to suppress the *tpm1Δ* defect (data not shown). Although more characterization of the domain is required to establish its function, these results suggest the possibility that the conserved domain interacts with an element of actin cytoskeleton. The La proteins have RNA-recognition motifs and the domain for homodimerization, which are distinct from the domain conserved with Sro9p (YOO and WOLIN 1994; CRAIG *et al.* 1997). The La protein binds the sequence UUU_{OH}, which is the 3′ terminus of most newly synthesized RNA polymerase III transcripts (STEFANO 1984). Genetic analysis using the yeast La-protein homologue, *LHP1* provides evidence that Lhp1p functions in pre-tRNA processing (YOO and WOLIN 1997). However, the biological roles of the domain conserved with Sro9p remains unknown. Intracellular distribution of RNA is important for cells; for example, asymmetric distribution of mRNA is essential for development of eggs (MICKLEM 1995; STEBBINGS *et al.* 1995). It is reported that asymmetric distribution of *oskar* RNA, which is critical for Drosophila development, requires tropomyosin (ERDELYI *et al.* 1995; TETZLAFF *et al.* 1996). In this context, it is interesting that the La proteins possess both an RNA-binding moiety and the domain that may be required for Sro9p to compensate loss of tropomyosin function. The genetic interaction between *SRO9* and tropomyosin genes may present a new aspect of the function of the La homology domain found in Sro9p.

We thank A. BRETSCHER for plasmids for tropomyosin, D. G. DRUBIN for *act1* mutant strains, G. JOHNSTON for a *myo2-66* mutant strain, I. MABUCHI for rabbit actin and helpful discussion, and A. NAKANO for helpful discussion. Part of this work was supported by a grant for scientific work from Monbusho; M.K. is a recipient of Fellowship of Japan Society for the Promotion of Science for Japanese Junior Scientists.

LITERATURE CITED

ADAMS, A. E. M., and J. R. PRINGLE, 1984 Relationship of actin and tubulin distribution to bud growth in wild-type and morphogenetic-mutant *Saccharomyces cerevisiae*. J. Cell Biol. **98:** 934–945.

BENDER, A., and J. R. PRINGLE, 1991 Use of a screen for synthetic lethal and multicopy suppressee mutants to identify two new genes involved in morphogenesis in *Saccharomyces cerevisiae*. Mol. Cell. Biol. **11:** 1295–1305.

BENDER, L., H. S. LO, H. LEE, V. KOKOJAN, J. PETERSON *et al.*, 1996 Associations among PH and SH3 domain-containing proteins and Rho-type GTPases in yeast. J. Cell Biol. **133:** 879–894.

BRETSCHER, A., B. DREES, E. HARSAY, D. SCHOTT and T. WANG, 1994 What are the basic functions of microfilaments? Insights from studies in budding yeast. J. Cell Biol. **126:** 821–825.

CARLSON, M., and D. BOTSTEIN, 1982 Two differentially regulated mRNAs with different 5′ ends encode secreted and intracellular forms of yeast invertase. Cell **28:** 145–154.

CHENEVERT, J., K. CORRADO, A. BENDER, J. PRINGLE and I. HERSKOWITZ, 1992 A yeast gene (*BEM1*) necessary for cell polarization whose product contains two SH3 domains. Nature **356:** 77–79.

CRAIG, A. W., Y. V. SVITKIN, H. S. LEE, G. J. BELSHAM and N. SONENBERG, 1997 The La autoantigen contains a dimerization domain that is essential for enhancing translation. Mol. Cell. Biol. **17:** 163–169.

CUMMINS, P., and S. V. PERRY, 1974 Chemical and immunological characteristics of tropomyosins from striated and smooth muscle. Biochem. J. **141:** 43–49.

DREES, B., C. BROWN, B. G. BARRELL and A. BRETSCHER, 1995 Tropomyosin is essential in yeast, yet the *TPM1* and *TPM2* products perform distinct functions. J. Cell Biol. **128:** 383–392.

ERDELYI, M., A. M. MICHON, A. GUICHET, J. B. GLOTZER and A. EPHRUSSI, 1995 Requirement for *Drosophila* cytoplasmic tropomyosin in *oskar* mRNA localization. Nature **377:** 524–527.

FIELD, C., and R. SCHEKMAN, 1980 Localized secretion of acid phosphatase reflects the pattern of cell surface growth in *Saccharomyces cerevisiae*. J. Cell Biol. **86:** 123–128.

GIETZ, R. D., and A. SUGINO, 1988 New yeast-*Escherichia coli* shuttle vectors constructed with *in vitro* mutagenized yeast genes lacking six-base pair restriction sites. Gene **74:** 527–534.

GUAN, K., and J. E. DIXON, 1991 Eukaryotic proteins expressed in *Escherichia coli*: an improved thrombin cleavage and purification procedure of fusion proteins with glutathione *S*-transferase. Anal. Biochem. **192:** 262–267.

HALL, A., 1992 Ras-related GTPases and the cytoskeleton. Mol. Biol. Cell **3:** 475–479.

HALL, A., 1994 Small GTP-binding proteins and the regulation of the actin cytoskeleton. Annu. Rev. Cell Biol. **10:** 31–54.

IMAI, J., A. TOH-E and Y. MATSUI, 1996 Genetic analysis of the *Saccharomyces cerevisiae RHO3* gene, encoding a Rho-type small GTPase, provides evidence for a role in bud formation. Genetics **142:** 359–369.

ITO, H., Y. FUKUDA, K. MURATA and A. KIMURA, 1983 Transformation of intact yeast cells treated with alkali cations. J. Bacteriol. **153:** 163–168.

JOHNSON, D. I., and J. R. PRINGLE, 1990 Molecular characterization of *CDC42*, a *Saccharomyces cerevisiae* gene involved in the development of cell polarity. J. Cell Biol. **111:** 143–152.

KENAN, D. J., C. C. QUERY and J. D. KEENE, 1991 RNA recognition: towards identifying determinants of specificity. Trends Biochem. Sci. **16:** 214–220.

KILMARTIN, J. V., and A. E. M. ADAMS, 1984 Structural rearrangements of tubulin and actin during the cell cycle of the yeast Saccharomyces. J. Cell Biol. **98:** 922–933.

KYTE, J., and R. F. DOOLITTLE, 1982 A simple method for displaying the hydropathic character of a protein. J. Mol. Biol. **157:** 105–132.

LEEUW, T., A. FOUREST-LIEUVIN, C. WU, J. CHENEVERT, K. CLARK *et al.*, 1995 Pheromone response in yeast: association of Bem1p with proteins of the MAP kinase cascade and actin. Science **270:** 1210–1213.

LIU, H., and A. BRETSCHER, 1989 Disruption of the single tropomyosin gene in yeast results in the disappearance of actin cables from the cytoskeleton. Cell **57:** 233–242.

LIU, H., and A. BRETSCHER, 1992 Characterization of *TPM1* disrupted yeast cells indicates an involvement of tropomyosin in directed vesicular transport. J. Cell Biol. **118:** 285–299.

MACK, D., K. NISHIMURA, B. K. DENNEHEY, T. ARBOGAST, J. PARKINSON *et al.*, 1996 Identification of the bud emergence gene *BEM4* and its interactions with Rho-type GTPases in *Saccharomyces cerevisiae.* Mol. Cell. Biol. **16:** 4387–4395.

MADAULE, P., R. AXEL and A. M. MYERS, 1987 Characterization of two members of the rho gene family from the yeast Saccharomyces cerevisiae. Proc. Natl. Acad. Sci. USA **84:** 779–783.

MANIATIS, T., E. F. FRITSCH and J. SAMBROOK, 1982 *Molecular Cloning: A Laboratory Manual.* Cold Spring Harbor Laboratory, Cold Spring Harbor, NY.

MATSUI, Y., and A. TOH-E, 1992a Isolation and characterization of two novel *ras* superfamily genes in *Saccharomyces cerevisiae.* Gene **114:** 43–49.

MATSUI, Y., and A. TOH-E, 1992b Yeast *RHO3* and *RHO4 ras* superfamily genes are necessary for bud growth, and their defect is suppressed by a high dose of bud formation genes *CDC42* and *BEM1.* Mol. Cell. Biol. **12:** 5690–5699.

MATSUI, Y., R. MATSUI, R. AKADA and A. TOH-E, 1996 Yeast *src* homology region 3 domain-binding proteins involved in bud formation. J. Cell Biol. **133:** 865–878.

MICKLEM, D. R., 1995 mRNA localization during development. Dev. Biol. **172:** 377–395.

NISHIKAWA, S., N. UMEMOTO, Y. OHSUMI, A. NAKANO and Y. ANRAKU, 1990 Biogenesis of vacuolar membrane glycoproteins of yeast *Saccharomyces cerevisiae.* J. Biol. Chem. **265:** 7440–7448.

NOVICK, P., and D. BOTSTEIN, 1985 Phenotypic analysis of temperature-sensitive yeast actin mutants. Cell **40:** 405–416.

NOVICK, P., and R. SCHEKMAN, 1979 Secretion and cell surface growth are blocked in a temperature-sensitive mutant of *Saccharomyces cerevisiae.* Proc. Natl. Acad. Sci. USA **76:** 1858–1862.

OLIVER, S. G., Q. J. VAN DER AART, M. L. AGOSTONI-CARBONE, M. AIGLE, L. ALBERGHINA *et al.*, 1992 The complete DNA sequence of yeast chromosome III. Nature **357:** 38–46.

PARAVICINI, G., M. COOPER, L. FRIEDLI, D. J. SMITH, J. L. CARPENTER *et al.*, 1992 The osmotic integrity of the yeast cell requires a functional *PKC1* gene product. Mol. Cell. Biol. **12:** 4896–4905.

PRINGLE, J. R., R. A. PRESTON, A. E. M. ADAMS, T. STEARNS, D. G. DRUBIN *et al.*, 1989 Fluorescence microscopy methods for yeast. Methods Cell Biol. **31:** 357–435.

RIDLEY, A. J., 1995 *Rho*-related proteins: actin cytoskeleton and cell cycle. Curr. Opin. Genet. Dev. **5:** 24–30.

SAIKI, R. K., D. H. GELFAND, S. STOFFEL, S. L. SCHARF, R. HIGUCHI *et al.*, 1988 Primer-directed enzymatic amplification of DNA with a thermostable DNA polymerase. Science **239:** 487–491.

SALMINEN, A., and P. J. NOVICK, 1987 A *ras*-like protein is required for a post-Golgi event in yeast secretion. Cell **49:** 527–538.

SHERMAN, F., G. R. FINK and J. B. HICKS, 1986 *Methods in Yeast Genetics.* Cold Spring Harbor Laboratory Press, Cold Spring Harbor, NY.

SHIRAYAMA, M., Y. MATSUI and A. TOH-E, 1995 The yeast *TEM1* gene, which encodes a GTP-binding protein, is involved in termination of M phase. Mol. Cell. Biol. **14:** 7476–7482.

SIKORSKI, R. S., and P. HIETER, 1989 A system of shuttle vectors and yeast host strains designed for efficient manipulation of DNA in *Saccharomyces cerevisiae.* Genetics **122:** 19–27.

STEBBINGS, H., J. D. LANE and N. J. TALBOT, 1995 mRNA translocation and microtubules: insect ovary models. Trends Cell Biol. **5:** 361–365.

STEFANO, J. E., 1984 Purified lupus antigen La recognizes an oligouridylate stretch common to the 3′ termini of RNA polymerase III transcripts. Cell **36:** 145–154.

TAKAI, Y., T. SASAKI, K. TANAKA and H. NAKANISHI, 1995 *Rho* as a regulator of the cytoskeleton. Trends Biochem. Sci. **20:** 227–231

TETZLAFF, M. T., H. JÄCKLE and M. J. PANKRATZ, 1996 Lack of *Drosophila* cytoskeletal tropomyosin affects head morphogenesis and the accumulation of *oskar* mRNA required for germ cell formation. EMBO J. **15:** 1247–1254.

TKACZ, J. S., and J. O. LAMPEN, 1972 Wall replication in Saccharomyces species: use of fluorescein-conjugated concanavalin A to reveal the site of mannan insertion. J. Gen. Microbiol. **72:** 243–247.

VIEIRA, J., and J. MESSING, 1987 Production of single-stranded plasmid DNA. Methods Enzymol. **153:** 3–9.

WELCH, M. D., D. A. HOLTZMAN and D. G. DRUBIN, 1994 The yeast actin cytoskeleton. Curr. Opin. Cell Biol. **6:** 110–119.

YOO, C. J., and S. L. WOLIN, 1994 La proteins from *Drosophila melanogaster* and *Saccharomyces cerevisiae*: a yeast homolog of the La autoantigen is dispensable for growth. Mol. Cell. Biol. **14:** 5412–5424.

YOO, C. J., and S. L. WOLIN, 1997 The yeast La protein is required for the 3′ endonucleolytic cleavage that matures tRNA precursors. Cell **89:** 393–402.

Communicating editor: F. WINSTON